# Molecular Dynamics in Physiological Solutions: Force-fields, Alkali Metal Ions, and Ionic Strength.

Chao Zhang,[†] Simone Raugei,[‡] Bob Eisenberg,[§] and Paolo Carloni[*,¶,‖]

*German Research School for Simulation Sciences, FZ-Juelich/RWTH Aachen University, Germany., Pacific Northwest National Laboratory, Richland, WA., Rush University Medical Center, Chicago, IL., and SISSA, Trieste, Italy; CNR-INFN-DEMOCRITOS, Trieste, Italy; Italian Institue of Technology (IIT), SISSA Unit, Trieste, Italy*

E-mail: p.carloni@grs-sim.de

**Abstract**

The monovalent ions $Na^+$ and $K^+$ and $Cl^-$ are present in any living organism. The fundamental thermodynamic properties of solutions containing such ions is given as the excess (electro-)chemical potential differences of single ions at finite ionic strength. This quantity is key for many biological processes, including ion permeation in membrane ion channels and DNA/protein interaction. It is given by a chemical contribution, related to the ion activity, and an electric contribution, related to the Galvani potential of the water/air interface. Here we investigate molecular dynamics based predictions of these quantities by using a variety of ion/water force-fields commonly used in biological simulation, namely the AMBER (the newly

[†]German Research School for Simulation Sciences, FZ-Juelich/RWTH Aachen University, Germany.
[‡]Pacific Northwest National Laboratory, Richland, WA.
[§]Rush University Medical Center, Chicago, IL.
[¶]SISSA, Trieste, Italy; CNR-INFN-DEMOCRITOS, Trieste, Italy; Italian Institue of Technology (IIT), SISSA Unit, Trieste, Italy
[‖]Current address: German Research School for Simulation Sciences, FZ-Juelich/RWTH Aachen University, Germany

developed), CHARMM, OPLS, Dang95 with TIP3P and the SPC/E water. Comparison with experiment is made with the corresponding values for salts, for which data are available. The calculations based on the newly developed AMBER force-field with the TIP3P water agrees well with experiment for both KCl and NaCl electrolytes in water solutions, as previously reported. The simulations based on the CHARMM-TIP3P and Dang95-TIP3P force-fields agree well for for the KCl and NaCl solutions, respectively. The other models are not as accurate. Single cations excess (electro-)chemical potential differences turn out to be similar for all the force-fields considered here. In the case of KCl, the calculated electric contribution is consistent with higher level calculations. Instead, such agreement is not found with NaCl. Finally, we found that the calculated activities for single $Cl^-$ ions turn out to depend clearly on the type of counter-ion used, with all the force-fields investigated. The implications of these findings for biomolecular systems are discussed.

# 1 Introduction

Monovalent ions such as $Na^+$ and $K^+$ and $Cl^-$ are essential to life. For example, the name of the channel protein that conducts these ions across the membranes of cells is often given by its selectivity for singe ions (*e.g.*, sodium channel, potassium channel, chloride channels). All living processes occur in the presence of the electrolyte solution with finite ionic strength: solutions outside cells are mostly $Na^+$ (about 0.14 molal or m[1]) and inside cells mostly $K^+$ (0.14 m) and $Cl^-$ (0.1 m).[2] Ions move through selective channels,[3] where local ionic strength can be as large as 5 m,[4,5] and rearrange dramatically in the formation of protein-, DNA- and RNA-protein complexes.[6–8] Therefore, the thermodynamics of *single ions* in the electrolyte solution at *finite ionic strength I* is of great interest for biological systems.

As we know from experiments, thermodynamic properties of electrolyte solutions at moderate $I$ (say 0.2 m) differ already from the ideal properties found at $I$=0. Indeed, ions like $Na^+$ and $K^+$ differ because they are non-ideal. They have even more dramatically non-ideal behavior at molal ionic strength.[9] The key quantity describing the non-ideal behavior of single ions in ionic solution

is the difference in excess (electro-) chemical potential ($\mu_X^{\mathrm{ex}}$, X=$Na^+$ , $K^+$ and $Cl^-$ ) between solutions at finite $I$ and those at $I$=0. This difference, which we write as $\Delta\mu_X^{I,\mathrm{ex}}$, is given by two contributions: (*i*) the chemical part, which accounts for the change of intermolecular interactions between the solution molecules/ions at finite $I$ compared to that at $I$=0;[10] (*ii*) the electrical part, which is due to the electrostatic potential inside the solution generated at the interface between air and any thermodynamically stable solution. This is the so-called Galvani potential.[11,12]

The calculation and the experimental determination of $\Delta\mu_X^{I,\mathrm{ex}}$ at finite $I$ are cumbersome. In fact, in molecular simulations approaches such as Monte-Carlo or molecular dynamics, one has to apply periodic boundary conditions to mimic macroscopic solutions: in these conditions, the non-negligible contribution due to the Galvani potential must be added.[13,14] Although this quantity is defined mathematically unambiguously, it can be calculated only in an approximate way, because of the well known limitations of sampling and force field accuracy in molecular simulations.[15,16] In addition, approximations must be necessarily introduced in the calculations of long-range electrostatics.[17–19] Experimentally, it is not possible to separate the contribution of an ion from that of its counter-ion(s) because experiments are necessarily carried out on neutral macroscopic systems. Extra-thermodynamic assumptions are then necessary.[20–23] Indirect estimates are obtained by an analysis of different salts.[24] Further complications might arise from deviations from ideal conditions, which are usually assumed.[11,12] These consider the ions as point particles, independent of size and chemical types of the ions, and the solution-air interface independent of boundary conditions.[25] In fact, the Galvani potential is likely to depend on the size and chemical nature of the particle. This fact is important for both theoretical and experimental estimates. Next, for the latter, the Galvani potential may depend also on complex effects specific to the setups. In particular, the thermodynamic properties of the interface may depend on finite-size effects and the presence of boundaries. Finally, in some experimental setups, non-equilibrium effects might be involved if flows are too slow to equilibrate on the time scale of experiments. The last two issues would arise in molecular simulation of the same setups.

Here we investigate the variance among force-fields in predictions of $\Delta\mu_X^{I,ex}$ of KCl and NaCl in

aqueous solution as well as the dependence of the predicted properties of $Cl^-$ ion on its $Na^+$ or $K^+$ counter-ions. To this end, we performed molecular dynamics simulation of the ions in solutions based on a variety of force-fields commonly used in biomolecular simulations. These include the AMBER[26] (the newly developed), CHARMM,[27,28] OPLS[29] and Dang95[30] in combination with SPC/E[31] and the TIP3P[32] water models.

Prior of the prediction of $\Delta\mu_X^{I,ex}$, we explore the domain of applicability of these force-fields. This is a nontrivial issue as these potentials are commonly calibrated by fitting to quantities like ion hydration free energy at $I$=0 or the first peak of ion-water radial distribution functions, which are not sensitive to $I$.[33] This means that the non-ideal effects of ions at finite strength are not considered in the parametrization. Because this issue cannot be addressed by considering $\Delta\mu_X^{I,ex}$ for the reasons outlined above, we resort here to a comparison between the predicted and experimental values for NaCl and KCl salts, $\Delta\mu_{NaCl}^{I,ex}$ and $\Delta\mu_{KCl}^{I,ex}$. For these, the contribution from the Galvani potential vanishes.[14,23] Therefore, the properties of the air/water are not involved in the evaluation of electrostatics. This makes the calculation straightforward. In addition, experimental values are available for neutral salts solutions, such as KCl and NaCl solutions.[34] So far, such comparison has been made with the newly developed AMBER force-field and TIP3P water solutions.[26] It is extended here to the other force-fields listed above.

Our paper is organized as follows. Section 2 reports the thermodynamic quantities of interest in this work and the computational details. Section 3.1 assesses the accuracy of the force-fields by a comparison of calculated and experimental values for $\Delta\mu_{NaCl}^{I,ex}$ and $\Delta\mu_{KCl}^{I,ex}$. Section 3.2 reports our estimate of $\Delta\mu_X^{I,ex}$ (X=$Na^+$ , $K^+$ and $Cl^-$ ), while Section 3.3 reports the calculated electrical contributions to $\Delta\mu_{Na^+}^{I,ex}$ and $\Delta\mu_{K^+}^{I,ex}$, for which corresponding values obtained by higher level calculations are available. Section 3.4 describes the dependence of the chemical contribution to $\Delta\mu_{Cl^-}^{I,ex}$ from the type of counter-ion. Section 4 discusses the implications of our results for biological systems. Section 5 summarizes the results.

# 2 Theory and Methods

## 2.1 Definition of excess (electro-)chemical potential difference $\Delta\mu_X^{I,ex}$

The (electro-)chemical potential of a monovalent ion X at finite $I$, $\mu_{\mathrm{X}}^I$, can be expressed as:[23,35]

$$\mu_{\mathrm{X}}^I = \mu_{\mathrm{X}}^\circ + RT\ln\frac{I}{I^\circ} + RT\ln\gamma_{\mathrm{X}} + zF\varphi^I, \tag{1}$$

The reference chemical potential $\mu_{\mathrm{X}}^\circ$ is defined as the chemical potential of the X ion (*e.g.*, $Na^+$) in an infinitely diluted solution (*i.e.*, its ionic strength $I^\circ \to 0$) of one of its salts (*e.g.*, NaCl) at room temperature and 1 atm pressure.

$\gamma_{\mathrm{X}}$ is the activity coefficient of X. It characterizes the non-ideal thermodynamic behavior of ions due to ion-ion and ion-water interactions at at finite $I$. $\gamma_X$ is assumed to be 1 in the reference state. $RT\ln\gamma_{\mathrm{X}}$, is usually referred to as the chemical contribution to $\mu_{\mathrm{X}}^I$.

$\varphi^I$ is the Galvani potential at finite $I$. It arises by bringing an ion from an infinite distance into the interior of the liquid phase.[11] $z$ is charge number (*e.g.*, $z = 1$ for $Na^+$). $zF\varphi^I$ includes two parts: (i) the contribution of the Volta potential, which vanishes if the solution bears no net charge (as in our case);[23] (ii) The contribution due to the surface potential generated by the specific dipole orientation of water molecules and their quadrupole moments at the solution interface.[36–38] This provides a non-negligible contribution to $\mu_{\mathrm{X}}^I$ [14,23] .

The excess (electro-) chemical potential which accounts for the intermolecular interaction between solution molecule/ions, is defined as:[10]

$$\mu_{\mathrm{X}}^{I,ex} = \mu_{\mathrm{X}}^{\circ,ex} + RT\ln\gamma_{\mathrm{X}} + zF(\varphi^I - \varphi^\circ), \tag{2}$$

$\mu_{\mathrm{X}}^{\circ,ex}$ is the excess (electro-)chemical potential of the reference state or the hydration free energy of ions, whereas $\varphi^\circ$ is the Galvani potential of liquid water.

The excess (electro-)chemical potential difference is then given by difference between $\mu_{\mathrm{X}}^{I,ex}$

and $\mu_{\mathrm{X}}^{\circ,ex}$

$$\Delta\mu_{\mathrm{X}}^{I,ex} = RT\ln\gamma_{\mathrm{X}} + zF(\varphi^I - \varphi^\circ), \tag{3}$$

The practical calculation of $zF(\varphi^I - \varphi^\circ)$ poses some challenges. It is presented in the next Section, along with the straightforward calculation of $RT\ln\gamma_{\mathrm{X}}$.

The excess (electro-)chemical potential of a salt (*e.g.*, NaCl) is easily obtained from the arithmetic average of the contributions from cations and anions:

$$\Delta\mu_{NaCl}^{I,ex} = (\Delta\mu_{\mathrm{Na}^+}^{I,ex} + \Delta\mu_{\mathrm{Cl}^-}^{I,ex})/2 \tag{4}$$

Notice that the contribution due to the Galvani potential to $\Delta\mu_{NaCl}^{I,ex}$ and to $\Delta\mu_{KCl}^{I,ex}$ is zero because the electrolyte itself is neutral, even though its component ions are not. In fact $zF(\varphi^I - \varphi^\circ)$ of $\mathrm{Na}^+$ (or $\mathrm{K}^+$) has the opposite sign of $zF(\varphi^I - \varphi^\circ)$ of $\mathrm{Cl}^-$.

## 2.2 Calculation of the chemical contribution to $\Delta\mu_X^{I,ex}$

$RT\ln\gamma_{\mathrm{X}}$ has been calculated here from well-known thermodynamic integration (TI) approach[39–41] and its replica-exchange variant.[42–44]

In the TI approach, the Hamiltonian of our initial systems (*e.g.*, the NaCl or KCl solutions at a given ionic strength $I$) is gradually perturbed by inserting an ion $X$ and the free energy difference between the initial system and final system is then calculated. The perturbation is commonly divided into smaller windows by varying the coupling parameter $\lambda$ from 0 to 1 in the Hamiltonian:

$RT\ln\gamma_{\mathrm{X}}$ is then obtained by numerical integration of each $\lambda$ window.

$$RT\ln\gamma_{\mathrm{X}} = -\frac{1}{\beta}\ln\int_0^1 d\lambda\,\langle U^I\rangle_{I,\lambda} + \frac{1}{\beta}\ln\int_0^1 d\lambda\,\langle U^\circ\rangle_{\circ,\lambda} \tag{5}$$

Here, $U$ is the binding energy of the ion with the initial system. $\langle U\rangle_\lambda$ is the ensemble average of the thermodynamic force in each $\lambda$ window.

As expected,[14,26] the calculation of $\int_0^1 d\lambda\,\langle U^\circ\rangle_{\circ,\lambda}$ converges very well and $\sim 1$ ns of dynamics

was indeed sufficient to obtain excellent convergence. Instead, the calculation of $\int_0^1 d\lambda \left\langle U^I \right\rangle_{I,\lambda}$ turned out not to converge on the same time scale. This slow convergence may be caused by many reasons, including the fact that ion-pairing is non-zero at finite $I$[45] and that the diffusion of ions is slower at finite $I$.[46,47] Thus, starting with different initial locations of the ion may give different results. Because of these difficulties in convergence and stability of simulations, we adopted the replica-exchange variant of TI.[42–44] This is expected to converge much more efficiently.[43,44] In fact, this was the case here (See Supporting Info).

## 2.3 Calculation of the electrical contribution to $\Delta\mu_X^{I,ex}$

In molecular simulations with periodic boundary conditions, the air-liquid interface is absent. The contribution $zF(\varphi^I - \varphi^\circ)$ due to this interface potential is expected to be significant[48,49] and must be added. The magnitude of the interface potential depends on the details of the way long-range electrostatic calculations are calculated[13,50] In the conditions used here (P-sum or particle-based PME [51]), the interface potential can be estimated by molecular dynamics simulations of a liquid slab with vacuum interface[52–54] (See Section 2.5 for details).

## 2.4 Finite size correction to $\Delta\mu_X^{I,ex}$

Additionally, one should consider the finite size correction on the electrostatic energy to the free energy calculations:[17–19]

$$\frac{1}{2}q^2\left(1-\frac{1}{\varepsilon(0)}\right)\xi_{\mathrm{Ew}}, \tag{6}$$

where $q$ is the testing ion charge, $\varepsilon(0)$ is the static dielectric constant and $\xi_{\mathrm{Ew}} = -2.837297/L^3$, which comes from the Madelung constant for a simple cubic lattice. This correction is expected to be much smaller than the previous one for aqueous solutions.[55] Indeed, for our box size (about 6 nm, see next Section), it is expected to be 0.5 kJ/mol or smaller .[56]

Table 1: L-J parameters of ion models and the mixing rules

| Model | Atom | $\sigma$ (nm) | $\varepsilon$ (kJ/mol) | q (*e*) | Mixing rule |
|---|---|---|---|---|---|
| | $Na^+$ | 0.21595 | 1.47545 | 1.0 | |
| AMBER[26] | $K^+$ | 0.28384 | 1.79789 | 1.0 | Lorentz-Berthelot |
| (SPC/E) | $Cl^-$ | 0.48305 | 0.05349 | -1.0 | |
| | $Na^+$ | 0.24393 | 0.36585 | 1.0 | |
| AMBER[26] | $K^+$ | 0.30380 | 0.81041 | 1.0 | Lorentz-Berthelot |
| (TIP3P) | $Cl^-$ | 0.44776 | 0.14891 | -1.0 | |
| | $Na^+$ | 0.24299 | 0.19623 | 1.0 | |
| CHARMM[27,28] | $K^+$ | 0.31426 | 0.36401 | 1.0 | Lorentz-Berthelot |
| | $Cl^-$ | 0.40447 | 0.62760 | -1.0 | |
| | $Na^+$ | 0.33304 | 0.01160 | 1.0 | |
| OPLS[29] | $K^+$ | 0.49346 | 0.00137 | 1.0 | geometric |
| | $Cl^-$ | 0.44172 | 0.49283 | -1.0 | |
| | $Na^+$ | 0.25840 | 0.41840 | 1.0 | |
| Dang95[30] | $K^+$ | 0.33320 | 0.41840 | 1.0 | Lorentz-Berthelot |
| | $Cl^-$ | 0.44010 | 0.41840 | -1.0 | |
| SPC/E[31] | O | 0.31660 | 0.65060 | -0.8476 | |
| | H | 0.00 | 0.00 | 0.4238 | |
| TIP3P[32] | O | 0.31510 | 0.63640 | -0.834 | |
| | H | 0.00 | 0.00 | 0.417 | |
| | H[59,60] | 0.04000 | 0.19246 | 0.417 | |

## 2.5 Computational Details

All classical molecular dynamics simulations were performed using the GROMACS package.[57,58] Parameters and references are listed in Table 1.

Simulations were performed at the following ionic strength: 0.01 m, 0.15 m, 0.67 m, 1.39 m, 3.27 m, 4.28 m and 4.80 m for KCl aqueous solution; 0.01 m, 0.15 m, 0.67 m, 1.39 m, 3.27 m, 4.80 m, 5.56 m for the NaCl aqueous solution. The composition of the systems is listed in Table 2. An edge of 6.0 nm was chosen for the initial (cubic) simulation cell. This cell resulted to be large enough to yield a good statistics for ion pairs at low ionic strength and correct estimates of the bulk properties of water, such as the dielectric constant[61] (also see Supporting Info). Ions were randomly placed inside water box with separation longer than 0.45 nm. Each system was equilibrated for 1 ns with timestep of 2 fs in a Nośe-Hoover thermostat[62,63] at 298 K and Parrinello-Rahman barostat[64] at 1 bar. PME method[51] was used to treat the long-range electrostatic interaction in peri-

odic system. Medium high accuracy settings for PME were adopted,[65] in which the number of grid points for the reciprocal space calculation of the electrostatic energy calculation was 0.01 nm, a 6$^{th}$ degree B-spline interpolation was used and the width of the screening Gaussian charge $\eta$ was set to be 3.4 nm$^{-1}$. The van der Waals and short-range Coulomb interaction cutoff was 0.1 nm. The dispersion correction term was applied to the energy and pressure.[66] The SETTLE algorithm[67] was used for the rigid water models (namely TIP3P and SPC/E).

Table 2: Number of water $N_{water}$ and number of ion-pair $N_{ion-pair}$ in the simulation system

| Ionic strength (m) | 0.01 | 0.15 | 0.67 | 1.39 | 3.27 | 4.28 | 4.80 | 5.56 |
|---|---|---|---|---|---|---|---|---|
| $N_{water}$[68] | 7804 | 7764 | 7624 | 7436 | 6986 | 6766 | 6656 | 6504 |
| $N_{ion-pair}$ | 0 | 20 | 90 | 184 | 409 | 519 | 574 | 650 |

Free energy calculations were carried out in the NVT ensemble with a Nośe-Hoover thermostat[62,63] at 298 K, staring from the last frame of the equilibration run. A Two-stage[69] replica-exchange TI[42–44] was used to calculate the excess chemical potential. In the first stage, the ion was gradually neutralized, whereas in the second stage, the van der Waals interaction was slowly switched off. A soft-core potential was used to avoid singularity of force when testing whether an ion appeared or disappeared.[70] At each stage, 10 equispaced $\lambda$ windows were sampled. For each $\lambda$ window, simulations were started from uncorrelated configurations. Exchanges between neighboring $\lambda$ configurations were attempted every 3 ps. The first picosecond of each of these 3 ps simulations was discarded. A total of 2 ns long trajectories were collected for each replica-exchange TI stage. The trapezoid rule was used to integrate the averaged thermodynamics force profile. The statistical error of each window was estimated by block averaging[71] and the final error of the free energy difference was calculated by error propagation.

The calculation of the surface potential was carried out in an orthorhombic cell in a 8.4 nm thick slab containing water and ions in the same composition as used in the free energy calculation. The spacing along the z-axis was large enough to create two vapor-liquid interfaces and 3D periodic boundary conditions were applied. The box size was chosen around 2.8 nm$\times$2.8 nm$\times$8.4 nm, as is usual in simulations of the surface potential of air-liquid interface.[48,49,52–54] Each simulation was performed for 10 ns in NVT ensemble with a Nośe-Hoover thermostat.[62,63] Electrostatic po-

tential was evaluated from the averaged charge density profile along the $z-$axis. The density was calculated on 0.02 nm grid.[72]

# 3 Result and Discussions

## 3.1 $\Delta\mu^{I,ex}_{KCl}$ and $\Delta\mu^{I,ex}_{NaCl}$ :Comparison between calculated values and experiment

Our calculated for salts $\Delta\mu^{I,ex}_{KCl}$ and $\Delta\mu^{I,ex}_{NaCl}$ using the newly developed AMBER-TIP3P force-field[26] reproduces quantitatively the experimental data (Figure 1), as previously reported.[73,74] The CHARMM-TIP3P and Dang95-SPC/E force-field based calculations predict accurately the values for the KCl and the NaCl solutions, respectively (Figure 2 ). All the other potential models are not as good (Figure 2). It is of interest to notice that a recent study[75] showed that the CHARMM parameters for Na-Cl interactions generated from the Lorentz-Berthelot combination rule lead to a larger underestimated of osmotic pressure - a probe for ions activity[12]- than the corresponding one for K-Cl interactions.

## 3.2 Calculation of $\Delta\mu^{I,ex}_{X}$

The calculated values for individual ions $\Delta\mu^{I,ex}_{X}$(X=$Na^+$, $K^+$ and $Cl^-$) are as scattered at finite $I$ as the corresponding ones for the KCl and NaCl salts (Figure 3). This hints that thermodynamics of ions using different force-fields differ from each other at finite $I$.

The magnitude of these values for $\Delta\mu^{I,ex}_{X}$ is comparable with that of the available experimentally derived data.[24] However, the calculated $\Delta\mu^{I,ex}_{K^+}$ increases with $I$ more than $\Delta\mu^{I,ex}_{Na^+}$. The opposite trend is found in the experimental estimates.[76] Similarly, the calculated $\Delta\mu^{I,ex}_{Cl^-}$ decreases with $I$ more in the KCl solution than it does in the NaCl solution. The opposite occurs for the experimentally derived values. These significant discrepancies may arise from several errors and assumptions from both theory and experiments, as discussed in the Introduction.

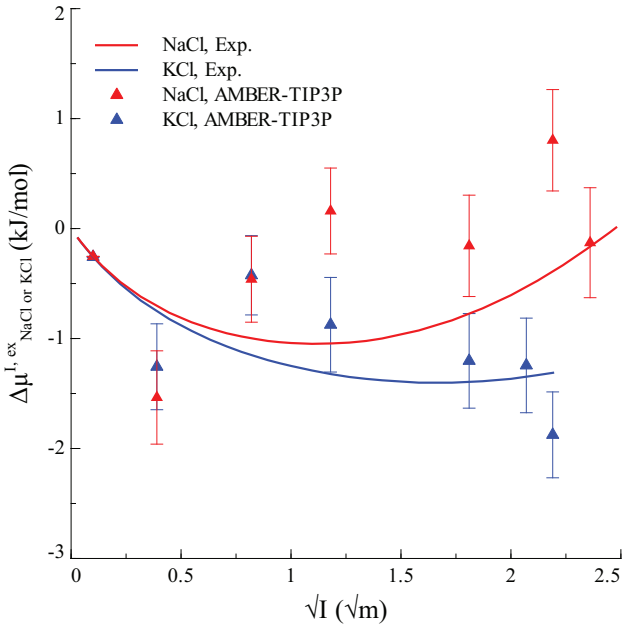


Figure 1: Calculated excess (electro-)chemical potential differences for KCl $\Delta\mu^{I,ex}_{KCl}$ and for NaCl $\Delta\mu^{I,ex}_{NaCl}$, based on the newly developed AMBER-TIP3P force-field,[26] plotted as a function of the square root of the molal ionic strength. Comparing is made with experimental data .[34]

To provide some hints of the origin of errors specific to the calculations, we focus here on comparisons against results obtained using higher level calculations. These are available only for the electrical contribution $zF(\varphi^I - \varphi^\circ)$.

## 3.3 Some considerations on the electrical contribution $zF(\varphi^I$-$\varphi^\circ)$

In this section, we report our calculated values for $zF(\varphi^I - \varphi^\circ)$ at finite $I$ and compare with previous calculations, based on polarizable force fields.[48,49] Notice that also the latter results, even though they are expected to be much more accurate than those based on non-polarizable force field, still cannot present the exact Galvani Potential. This is because they do not fully take into account the contribution due to the molecular quadrupoles.[36,37]

The calculated electrical contribution $zF(\varphi^I - \varphi^\circ)$ to $\Delta\mu^{I,ex}_{K^+}$ increases linearly with $I$ for all the force-fields used here, ranging from 0 to 16 kJ/mol (Figure 4) .[77,78] The range of the calculated values of $zF(\varphi^I - \varphi^\circ)$ is comparable to that obtained by polarizable ion/water force-fields based calculations at $I$=1 m (from 1 to 4 kJ/mol versus 3.4 kJ/mol).[48,79]

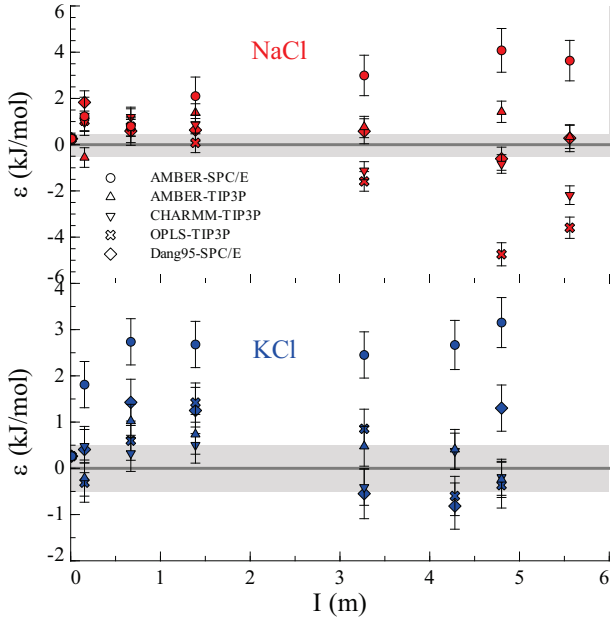


Figure 2: Deviations $\varepsilon$ of calculated excess (electro-)chemical potential differences for KCl $\Delta\mu^{I,ex}_{KCl}$ and for NaCl $\Delta\mu^{I,ex}_{NaCl}$ from experimental data[34] plotted as a function of the molal ionic strength. The shadow area covers the deviation $\varepsilon$ within $\pm$0.5 kJ/mol. The results obtained with all the force-fields considered in this work are presented.

The overall values of calculated $zF(\varphi^I - \varphi^\circ)$ for $Na^+$ range from -3 to 3 kJ/mol. Thus, the values of $zF(\varphi^I - \varphi^\circ)$ at $I$=1 m range from -1 to 0.5 kJ/mol, to be compared with the value obtained with a polarizable force-field of 3.5 kJ/mol.[49,79] We conclude that non-polarizable models for the NaCl solution are not able to reproduce the results of polarizable models.

The experiments estimated an increase of the Galvani potential in both KCl and NaCl electrolyte solution at finite $I$.[37,80,81] However the quantities are all much smaller (0.2 kJ/mol for the KCl[80,82] and 0.3 kJ/mol for the NaCl at $I$=1 m[80,82]). The very large discrepancies between theory and experiment reflect the difficulties in experimental measurement of the Galvani potential (see Introduction) as well as limitations of the molecular simulation methods outlined in the Introduction.

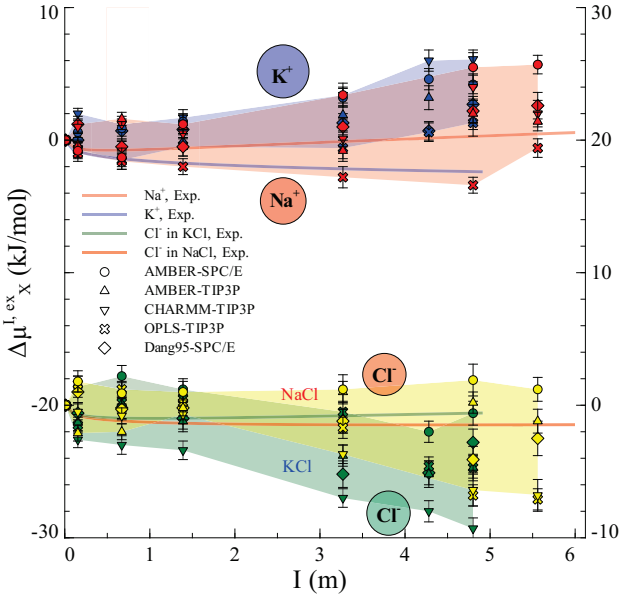


Figure 3: Calculated excess (electro-)chemical potential differences for single ions $\Delta\mu_X^{I,ex}$ (X=$Na^+$, $K^+$ and $Cl^-$) in KCl and NaCl solutions, plotted as a function of the molal ionic strength. The results obtained with all the force-fields considered in this work are presented. Experimentally derived estimates are also reported .[24]

## 3.4 $RT \ln \gamma_{Cl^-}$ :dependence from the types of counter-ions

The chemical contribution $RT \ln \gamma_{Cl^-}$ as a function of $I$ depends on the type of counter-ion for all the force-fields used here (Figure 5) .

As mentioned before, $RT \ln \gamma_{Cl^-}$ reflects the change of intermolecular interactions between $Cl^-$-ions and $Cl^-$-water at finite $I$. This change in electrolyte solution is often attributed to the electrostatic interactions as a first approximation.[83] We find the $Cl^-$- ion electrostatic contribution to $RT \ln \gamma_X$ of the NaCl solution is dramatically different from that of KCl solution, obtained from a calculation based on the newly developed AMBER-SPC/E force-field[26,84] (inset in Figure 5). Similar conclusions can be drawn for $Cl^-$- water electrostatic contributions in the two salt solutions (Data not shown).

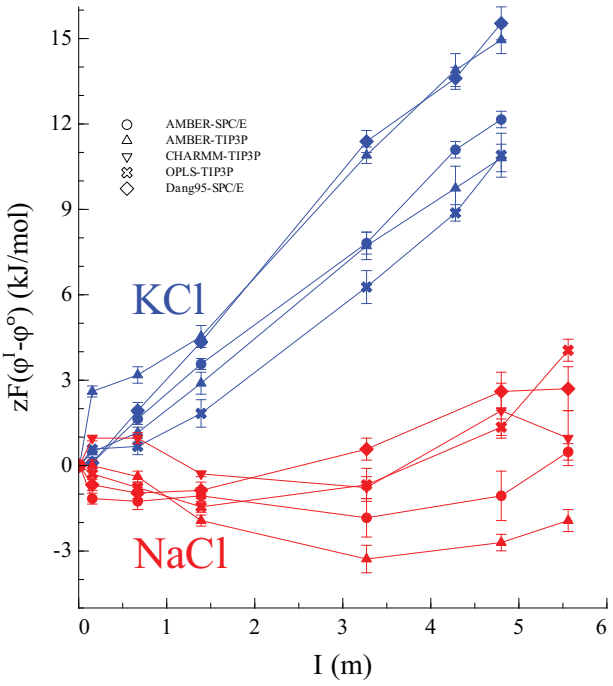


Figure 4: Calculated electrical contribution $zF(\varphi^I - \varphi^\circ)$ to $\Delta\mu_X^{I,ex}$ for $K^+$ and $Na^+$ in in KCl and NaCl respectively ($z = 1$), plotted as a function of the molal ionic strength $I$. The results obtained with all the force-fields considered in this work are presented.

# 4 Implication for biological systems

The success of predicting the values for salts is gratifying with some of the force-fields considered here, especially considering their very simple functional form. The success testifies to the care with which force-fields have been developed. However, the challenges reported previously[13,20–22,55,85] and addressed here, do remain in the prediction of $\Delta\mu_X^{I,ex}$ (X=$Na^+$, $K^+$ and $Cl^-$), and in particular of the electric contribution to it (See Section 2.3 and 3.3). These difficulties may be even larger when modeling biological systems. Such difficulties do not come without consequence. Consider the simple identification of an ion channel as done by (literally) thousands of laboratories every day. That identification depends on the measurement and identity of the (so called) reversal potential,[86,87] which is the experimental estimator of the gradient of chemical potential, or the equilibrium potential as it was called by Hodgkin and Huxley.[88,89] The name of the channel is often determined by its selectivity[90–93](*e.g.*, sodium channel, potassium channel, chloride channel) and that in turn depends on the identification of the reversal potential with the gradient of chemical

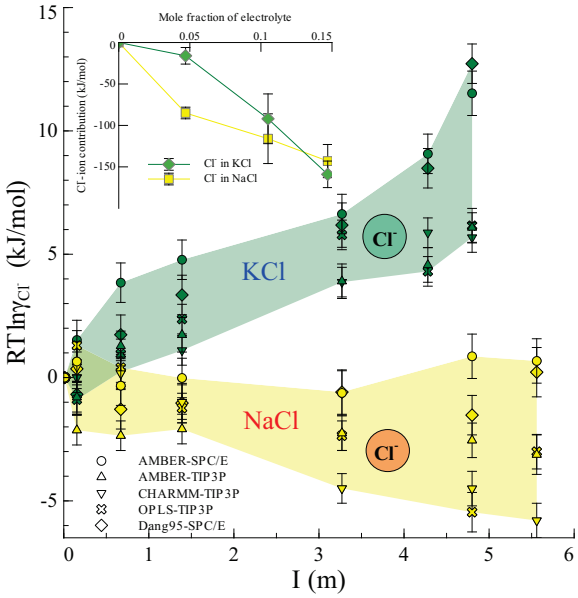


Figure 5: Calculated chemical contribution $RT \ln \gamma_{Cl^-}$ in KCl and NaCl aqueous solutions, plotted as a function of the molal ionic strength. The results obtained with all the force-fields considered in this work are presented. Inset: $Cl^-$- ion electrostatic contribution to $RT \ln \gamma_{Cl^-}$ based on the newly developed AMBER-SPC/E force-field.[26]

potential of one ion. If in fact $\Delta\mu_X^{I,ex}$ is not accurately included[94–98] in the calculation of the gradient of chemical potential (when using ionic strength of ions as inputs), the channel identification may be askew.[97]

The selectivity properties of ion channels are crucially important to their function. Ions that differ in their non-ideal properties—like $Na^+$ and $K^+$—carry different 'messages' (*i.e.*, signals) to different systems of the cell and so there is an enormous literature trying to measure, understand, simulate, control, and even synthesize[99–101] the selectivity of different types of channels. Estimates and computations of selectivity depend critically on estimates of $\Delta\mu_X^{I,ex}$, because many types of ions differ only because they are non-ideal. Similar considerations[87,102–113] are likely to apply to a myriad of other biological events. Many important biological properties arise because of the non-ideal properties of individual types of ions.

# 5 Conclusion

We have established the quality of a variety of standard ion/water force-fields commonly used in biological simulation, for the calculation of the excess (electro-)chemical potential for KCl $\Delta\mu^{I,ex}_{KCl}$ and for NaCl $\Delta\mu^{I,ex}_{NaCl}$. Specifically, the AMBER[26] (the newly developed), CHARMM,[27,28] OPLS[29] and Dang95[30] were considered in combination with SPC/E[31] and TIP3P[32] water models. The calculation based on the newly developed AMBER-TIP3P agrees well with the experimental values for both KCl and NaCl solutions, as previously reported.[73] Instead the CHARMM-TIP3P potential agrees well with the KCl salt, whereas the Dang95-SPC/E potential agrees well with the NaCl salt. The others potential models do not give good results for any of the two aqueous solution studied. Hence, care should be taken in biomolecular simulations when using these force-fields at physiological $I$.

The calculated $\Delta\mu^{I,ex}_{Na^+}$ values are similar to those of $\Delta\mu^{I,ex}_{K^+}$. The calculated values are as scattered at finite $I$ as the corresponding ones for the KCl and NaCl salts. Only the calculated electric contribution $zF(\varphi^I - \varphi^\circ)$ of $K^+$ is consistent with reported higher level calculations with polarizable ion/water force-fields.[48]

The calculated chemical contribution $RT \ln \gamma_{Cl^-}$ to $\Delta\mu^{I,ex}_{Cl^-}$ depends on the type of counter-ions present. This result may be of interest for force-field calculations of $Cl^-$-dependent biological systems (such as chloride channels[114])

# 6 Acknowledgement

The author (C. Z.) thanks F. Marinelli for helpful discussion on replica-exchange method. We thank the reviewers for their highly valuable comments on the manuscript.

# References

(1) “m” is molal scale not molar scale, *i.e.*, m is mol/1kg of $H_2O$.

(2) Costanzo, L. S. *Physiology*; Elsevier/Saunders: Philadelphia, 2006; pp 2–4.

(3) Gouaux, E.; MacKinnon, R. *Science* **2005**, *310*, 1461.

(4) Doyle, D. A.; Cabral, J. M.; Pfuetzner, R. A.; Kuo, A.; Gulbis, J. M.; Cohen, S. L.; Chait, B. T.; MacKinnon, R. *Science* **1998**, *280*, 69.

(5) Domene, C.; Vemparala, S.; Furini, S.; Sharp, K.; Klein, M. L. *J. Am. Chem. Soc* **2008**, *130*, 11.

(6) Jayaram, B.; Jain, T. *Annu. Rev. Biophys. Biomol. Struct.* **2004**, *33*, 343.

(7) Auffinger, P.; Hashem, Y. *Curr. Opin. Stru. Biol* **2007**, *17*, 325.

(8) Chu, V. B.; Bai, Y.; Lipfert, J.; Herschlag, D.; Doniach, S. *Curr. Opin. Chem. Biol*. **2008**, *12*, 619.

(9) Lee, L. L. *Molecular Thermodynamics of Electrolyte Solutions*; World Scientific: New York, 2008; pp 11–38.

(10) Beck, T. L.; Paulaitis, M. E.; Pratt, L. R. *The Potential Distribution Theorem and Models of Molecular Solutions*; Cambridge University Press: Cambridge, 2006; pp 45–68.

(11) Butt, H. J.; Graf, K.; Kappl, M. *Physics and Chemistry of Interfaces*; Wiley-VCH: Weinheim, 2006; pp 77–79.

(12) *Liquids, Solutions, and Interfaces: From Classical Macroscopic Descriptions to Modern Microscopic Details*; Fawcett, W. R., Ed.; Oxford University Press: New York, 2004; pp 3–147.

(13) Kastenholz, M. A.; Hünenberger, P. H. *J. Chem. Phys.* **2006**, *124*, 224501.

(14) Lamoureux, G.; Roux, R. *J. Phys. Chem. B* **2006**, *110*, 3308.

(15) van Gunsteren, W. F. et al. *Angew. Chem. Int. Ed.* **2006**, *45*, 4064.

(16) McDowell, S. E.; Spacková, N.; Sponer, J.; Walter, N. G. *Biopolymer* **2007**, *82*, 169.

(17) Hummer, G.; Pratt, L. R.; García, A. E. *J. Phys. Chem.* **1996**, *100*, 1206.

(18) Hummer, G.; Pratt, L. R.; Garcá, A. E. *J. Chem. Phys.* **1997**, *107*, 9275.

(19) Hünenberger, P. H.; McCammon, J. A. *J. Chem. Phys.* **1999**, *110*, 1856.

(20) Conway, B. E. *J. Sol. Chem.* **1978**, *7*, 720–770.

(21) Marcus, Y. *J. Chem. Soc. Faraday Trans.* **1987**, *83*, 2985.

(22) Tissandier, M. D.; Cowen, K. A.; Feng, W. Y.; Gundlach, E.; Cohen, M. H.; Earhart, A. D.; Coe, J. V. *J. Phys. Chem. A* **1998**, *102*, 7787.

(23) Fawcett, W. R. *Langmuir* **2008**, *24*, 9868.

(24) Wilczek-Vera, G.; Rodil, E.; Vera, J. H. *AIChE J.* **2004**, *50*, 445.

(25) Within these simplifying assumptions, the Galvani potential is the same for $K^+$, $Na^+$, and it is opposite in sign for $Cl^-$.

(26) Joung, I. S.; Cheatham, III, T. E. *J. Phys. Chem. B* **2008**, *112*, 9020.

(27) Beglov, D.; Roux, B. *J. Chem. Phys.* **1994**, *100*, 9050.

(28) Roux, B. *Biophys. J.* **1996**, *71*, 3177.

(29) Jorgensen, W. L.; Maxwell, D. S.; Tirado-Rives, J. *J. Am. Chem. Soc.* **1996**, *118*, 11225.

(30) Dang, L. X. *J. Am. Chem. Soc.* **1995**, *117*, 6954.

(31) Berendsen, H. J. C.; Grigera, J. R.; Straatsma, T. P. *J. Phys. Chem.* **1987**, *91*, 6269.

(32) Jorgensen, W. L.; Chandrasekhar, J.; Madura, J. D.; Impey, R. W.; Klein, M. L. *J. Chem. Phys.* **1983**, *79*, 926.

(33) Patra, M.; Karttunen, M. *J. Comput. Chem.* **2004**, *25*, 678.

(34) Hamer, W. J.; Wu, Y.-C. *J. Phys. Chem. Ref. Data.* **1972**, *1*, 1047.

(35) Fawcett, W. R. *Liquids, Solutions, and Interfaces: From Classical Macroscopic Descriptions to Modern Microscopic Details*; Oxford University Press: New York, 2004; pp 395–422.

(36) Paluch, M. *Adv. Colloid Interface Sci.* **2000**, *84*, 27.

(37) Petersen, P. B.; Saykally, R. J. *Annu. Rev. Phys. Chem.* **2006**, *57*, 333.

(38) Continuum models encounter difficulties in describing the Galvani potential because the latter depends on the polarization of the system.

(39) Kirkwood, J. G. *J. Chem. Phys.* **1935**, *3*, 300.

(40) Ferrrario, M.; Ciccoti, G.; Spohr, E.; Cartailler, T.; Turq, P. *J. Chem. Phys.* **2002**, *117*, 4947.

(41) *Free Energy Calculations*; Chipot, C., Pohorille, A., Eds.; Springer, 2007; pp 33–72.

(42) Fukunishi, H.; Watanabe, O.; Takada, S. *J. Chem. Phys.* **2002**, *116*, 9058.

(43) Woods, C. J.; Essex, J. W.; King, M. A. *J. Phys. Chem B* **2003**, *107*, 13711.

(44) Jiang, W.; Hodoscek, M.; Roux, B. *J. Chem. Theory Comput.* **2009**, *5*, 2583.

(45) Uchida, H.; Matsuoka, M. *Fluid Phase Equilib* **2004**, *219*, 49.

(46) Chowdhuri, S.; Chandra, A. *J. Chem. Phys.* **2001**, *115*, 3732.

(47) Instead, the diffusion of ions has no impact on the convergence of TI calculation at infinite dilution.

(48) Wick, C. D.; Dang, L. X.; Jungwirth, P. *J. Chem. Phys.* **2006**, *125*, 024706.

(49) Bauer, B. A.; Patel, S. *J. Chem. Phys.* **2010**, *132*, 024713.

(50) Kastenholz, M. A.; Hünenberger, P. H. *J. Chem. Phys.* **2006**, *124*, 124106.

(51) Sagul, C.; Darden, T. A. *Annu. Rev. Biophys. Biomol. Struct.* **1999**, *28*, 155.

(52) Feller, S. E.; Pastor, R. W.; Rojnuckarin, A.; Bogusz, S.; Brooks, B. R. *J. Phys. Chem.* **1996**, *100*, 17011.

(53) Sokhan, V. P.; Tildesley, D. J. *Mol. Phys.* **1997**, *92*, 625.

(54) Lamoureux, G.; Mackerell Jr., A. D.; Roux, B. *J. Chem. Phys.* **2003**, *119*, 5185.

(55) Cheng, J.; Sulpizi, M.; Sprik, M. *J. Chem. Phys.* **2009**, *131*, 154504.

(56) The calculated static dielectric constants $\varepsilon(0)$ of KCl and NaCl solution comparing with experimental data as a function of the molal ionic strength can be seen in Supporting Info Figure S2.

(57) van der Spoel, D.; Lindahl, E.; Hess, B.; Groenhof, G.; Mark, A. E.; Berendsen, H. J. C. *J. Comp. Chem.* **2005**, *26*, 1701.

(58) Hess, B.; Kutzner, C.; van der Spoel, D.; Lindahl, E. *J. Chem. Theory Comput.* **2008**, *4*, 435.

(59) MacKerell, Jr., A. D. et al. *J. Phys. Chem. B* **1998**, *102*, 3586.

(60) Modified TIP3P water in CHARMM.[59]

(61) Lin, Y.; Baumketner, A.; Deng, S.; Xu, Z.; Jacobs, D.; Cai, W. *J.Chem. Phys.* **2009**, *131*, 154103.

(62) Nośe, S. *J. Chem. Phys.* **1984**, *81*, 511.

(63) Hoover, W. G. *Phys. Rev. A* **1985**, *31*, 1695.

(64) Parrinello, M.; Rahman, A. *Phys. Rev. Lett.* **1980**, *45*, 1196.

(65) Essmann, U.; Perera, L.; Berkowitz, M. L.; Darden, T.; Lee, H.; Pedersen, L. G. *J. Chem. Phys.* **1995**, *103*, 8577.

(66) Allen, M. P.; Tildesley, D. J. *Computer Simulation of Liquids*; Oxford Science Publications: Oxford, 1987; pp 64–68.

(67) Miyamoto, S.; Kollman, P. A. *J. Comp. Chem.* **1992**, *13*, 952.

(68) Exact number depends on the water model and the salt type.

(69) Kollman, P. *Chem. Rev.* **1993**, *93*, 2395.

(70) Beutler, T. C.; Mark, A. E.; Van Schaik, R. C.; Gerber, P. R.; Van Gunsteren, W. F. *Chem. Phys. Lett.* **1994**, *222*, 529.

(71) Hess, B. *J. Chem. Phys.* **2002**, *116*, 209.

(72) Note that it is also possible to obtain the Galvani potential by creating a virtual air-solution interface with those snapshots from simulations of bulk solutions under PBC and then integrating the charge density.

(73) Joung, I. S.; Cheatham, III, T. E. *J. Phys. Chem. B* **2009**, *113*, 13279.

(74) Notice that the time-scale of our simulation is shorter than that of these authors.[73] They use straightforward TI instead of replica-exchange TI. The latter converges faster, See Figure S1 in Supporting Info.

(75) Luo, Y.; Roux, B. *J. Phys. Chem. Lett.* **2010**, *1*, 183.

(76) Similar trends were also founded experimentally[24] in the presence of an anion other than $Cl^-$.

(77) Table S1 in Supporting Info presents a comparison of $\varphi^\circ$ values, which is not crucial for the $\Delta\mu_X^{I,ex}$ but may be relevant as a reference.

(78) We only observed a slightly preference of the anions at the interface than cations in the simulations (See Figure S3 in Supporting Info).

(79) The actual values reported in Refs[48,49] are $(\varphi^I - \varphi^\circ)$. For the sake of clarity, here we report $zF(\varphi^I - \varphi^\circ)$, which is the quantity of interest here.

(80) Randles, J. E. *Phys. Chem. Liq.* **1977**, *7*, 107.

(81) Jungwirth, P.; Tobias, D. J. *Chem. Rev.* **2006**, *106*, 1259.

(82) Jarvis, N. J.; Scheiman, M. A. *J. Phys. Chem.* **1968**, *72*, 74.

(83) Wright, M. R. *An Introduction to Aqueous Electrolyte Solutions*; Wiley, 2007.

(84) We expect similar results for all the other force-fields as they have the same trend in Figure 5. However, free energy decomposition is force-field and path dependent.

(85) Harder, E.; Roux, B. *J. Chem. Phys.* **2008**, *129*, 234706.

(86) Hille, B. *Ionic Channels of Excitable Membranes, 3rd ed.*; Sinauer Associates Inc.: Sunderland, 2001; pp 1–19.

(87) Zuhlke, R. D.; Pitt, G. S.; Deisseroth, K.; Tsien, R. W.; Reuter, H. *Nature* **1999**, *399*, 159.

(88) Hodgkin, A.; Huxley, A.; Katz, B. *Arch. Sci. Physiol.* **1949**, *3*, 129.

(89) Hodgkin, A. *J. Physiol.* **1976**, *263*, 1.

(90) Conley, E. C. *The Ion Channel Facts Book. I. Extracellular Ligand-gated Channels;*; Academic Press: New York, 1996; pp 3–11.

(91) Conley, E. C. *The Ion Channel Facts Book. II. Intracellular Ligand-gated Channels*; Academic Press: New York, 1996; pp 3–20.

(92) Conley, E. C.; Brammar, W. *The Ion Channel Facts Book III: Inward Rectifier and Intercellular Channels*; Academic Press: New York, 2000; pp 3–21.

(93) Conley, E. C.; Brammar, W. *The Ion Channel Facts Book IV: Voltage Gated Channels;*; Academic Press: New York, 1999; pp 3–21.

(94) Barry, P. H. *Am. J. Physiol.* **1990**, *259*, S15.

(95) Barry, P. H. *Ann. Biomed. Eng.* **1994**, *22*, 218.

(96) Barry, P. H. *J. Neurosci. Methods* **1994**, *51*, 107.

(97) Barry, P. H. *Cell. Biochem. Biophys.* **2006**, *46*, 143.

(98) Ng, B.; Barry, P. H. *J. Neurosci. Methods* **1995**, *56*, 37.

(99) Miedema, H.; Meter-Arkema, A.; Wieregna, J.; Tang, J.; Eisenberg, B.; Nonner, W.; Hektor, H.; Gillespie, D.; Meijberg, W. *Biophys. J.* **2004**, *87*, 3137.

(100) Miedema, H.; Vrouenraets, M.; Wieregna, J.; Eisenberg, B.; Gillespie, D.; Meijberg, W.; Nonner, W. *Biophys. J.* **2006**, *91*, 4392.

(101) Vrouenraets, M.; Wieregna, J.; Meijberg, W.; Miedema, H. *Biophys. J.* **2006**, *90*, 1202.

(102) Berg, J. M. *Ann. Rev. Biophys. Biophys. Chem.* **1990**, *19*, 405.

(103) Berg, J. M. *J. Biol. Chem.* **1990**, *265*, 6513.

(104) Cantwell, M. A.; Di Cera, E. *J. Biol. Chem.* **2000**, *275*, 39827.

(105) Berg, J. M.; Godwin, H. A. *Ann. Rev. Biophys. Biomol. Struct.* **1997**, *26*, 357.

(106) Carnell, C. J.; Bush, L. A.; Mathews, F. S.; Di Cera, E. *Biophys. Chem.* **2006**, *121*, 177.

(107) De Gristofaro, R.; Fenton II, J. W.; Di Cera, E. *J. Mol. Biol.* **1992**, *226*, 263.

(108) Di Cera, E. *Biopolymer* **1994**, *34*, 1001.

(109) Doroshenko, P. A.; Kostyuk, P. G.; Lukyanetz, E. A. *Neurosci.* **1998**, *27*, 1073.

(110) Eisenberg, R. S. *J. Membr. Biol.* **1990**, *115*, 1.

(111) Lambers, T. T.; Mahieu, F.; Oancea, E.; Hoofd, L.; de Lange, F.; Mensenkamp, A. R.; Voets, T.; Nilinus, B.; Clapham, D. E.; Hoenderop, J. G.; Bindels, R. J. *EMBO J.* **2006**, *25*, 2978.

(112) Tripathy, A.; Xu, L.; Mann, G.; Meissner, G. *Biophys. J.* **1995**, *69*, 106.

(113) Vescovi, E. G.; Ayala, Y. M.; Di Cera, E.; Groisman, E. A. *J. Biol. Chem.* **1997**, *272*, 1440.

(114) Suzuki, M.; Morita, T.; Iwamoto, T. *Cell. Mol. Life. Sci.* **2006**, *63*, 12.

# Supporting Information

Chao Zhang, Simone Raugei, Bob Eisenberg, Paolo Carloni

*German Research School for Simulation Sciences, FZ-Juelich/RWTH Aachen University, Germany;*
*Statistical and Biological Physics sector, SISSA, Italy;*
*Rush University Medical Center, Chicago, IL*

## A Convergence of free-energy calculation

The convergence of the free-energy estimate was tested running simulations starting from different (uncorrelated) configurations, using different numbers of $\lambda$ windows and different sampling times. Specifically, $\left\langle U^I \right\rangle_{I,\lambda}^{LJ}$ and $\left\langle U^I \right\rangle_{I,\lambda}^{Q}$ contributions to free energy have been calculated using straightforward TI and its replica-exchange variant. For sake of simplicity, in the following only the results obtained for the newly developed AMBER-SPC/E potential [1] are discussed. Similar features are expected for the other force-fields.

As can be seen from Figure S1 (bottom, left panel), when using replica-exchange TI, the term $\left\langle U^I \right\rangle_{I,\lambda}^{LJ}$ turns out not to depend significantly on the initial configuration. Conversely, using straightforward TI results strongly depend on the initial configuration (Figure S1 (top, left panel). Similar conclusions are obtained for the term $\left\langle U^I \right\rangle_{I,\lambda}^{Q}$ (Data not shown). As a whole, the final free energy difference $-\frac{1}{\beta}\ln\int_0^1 d\lambda \left\langle U^I \right\rangle_{I,\lambda}$ can change as much as 5 kJ/mol changing the starting point of simulations using straightforward TI.

The dependence of the average from the number of $\lambda$ windows is reported in Figure S1 (right panel) for the term $\left\langle U^I \right\rangle_{I,\lambda}^{Q}$. We remark that this is the larger of the two contributions to the thermodynamic force $\left\langle U^I \right\rangle_{I,\lambda}$. As can be seen, 10 $\lambda$ windows are sufficient to have converged values using with replica-exchange TI. The same is not likely to be true for the straightforward TI.

## B Dielectric constants of ionic solutions

See Figure S2.

## C Estimates of the Galvani potential of pure water

See Table S1.

## D Density profiles of concentrated salt aqueous solutions

See Figure S3. Similar results apply for other force-fields used in the text (Data not shown).

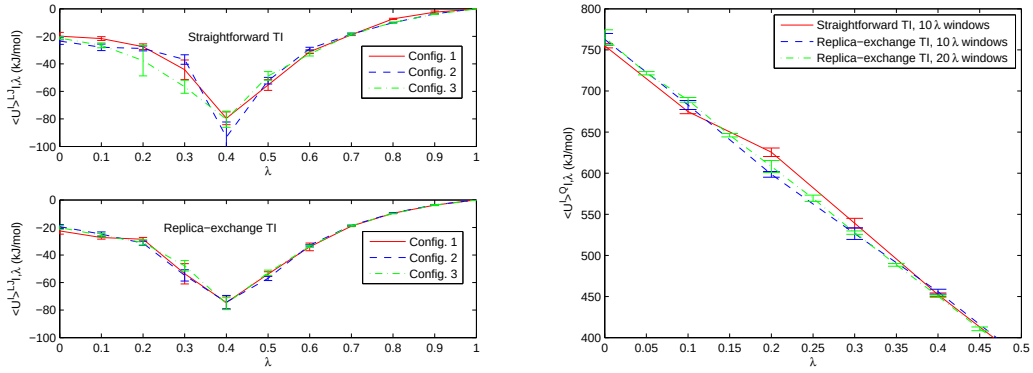


Figure S1: Ensemble averages of the Lennard-Jones potential contribution, $\left\langle U^I \right\rangle_{I,\lambda}^{LJ}$ (left), and the electrostatic interaction contribution, $\left\langle U^I \right\rangle_{I,\lambda}^{Q}$ (right), to the thermodynamic force $\left\langle U^I \right\rangle_{I,\lambda}$ for the KCl solution at 3.27m calculated for the newly developed AMBER-SPC/E potential [1]. Each contribution is calculated with both straightforward TI and replica-exchange TI, plotted as function of the coupling parameter $\lambda$. Comparison between different initial configurations and different numbers of $\lambda$ windows is made for $\left\langle U^I \right\rangle_{I,\lambda}^{LJ}$ and $\left\langle U^I \right\rangle_{I,\lambda}^{Q}$, respectively. In each point, the average is calculated over a 200 ps trajectory.

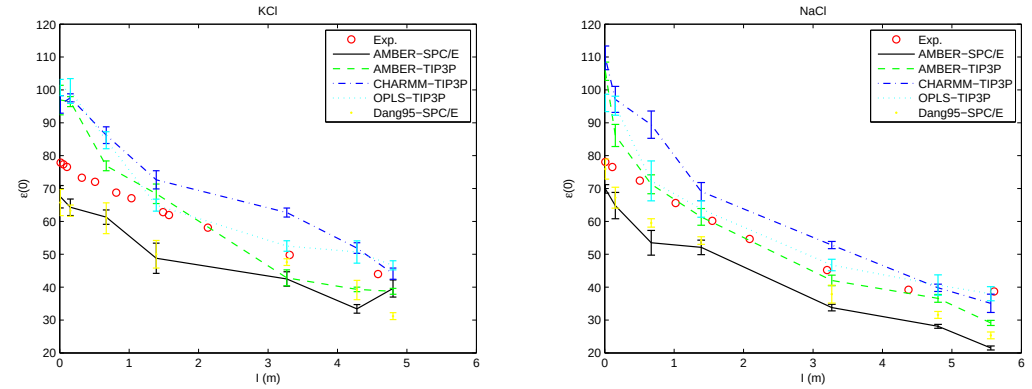


Figure S2: Calculated and experimental [2] static dielectric constant $\epsilon(0)$ as a function of the molal ionic strength $I$ for KCl and NaCl aqueous solutions.

Table S1: Estimates of the Galvani potential of pure liquid water $\varphi^\circ$ at 298 K. Results obtained in the present work are compared with previous calculations and experimental-derived values.

| | This Work | Ref. |
|---|---|---|
| SPC/E | -0.59V | -0.55V[3] |
| TIP3P | -0.52V | -0.52V[4], -0.50V[5] |
| DFT | – | 4V[6], -0.018V[7] |
| Exp. | – | 0.15V[8] |

# References

[1] I. S. Joung and T. E. Cheatham, III. Determination of alkali and halide monovalent ion parameters for use in explicitly solvated biomolecular simulations. *J. Phys. Chem. B,*

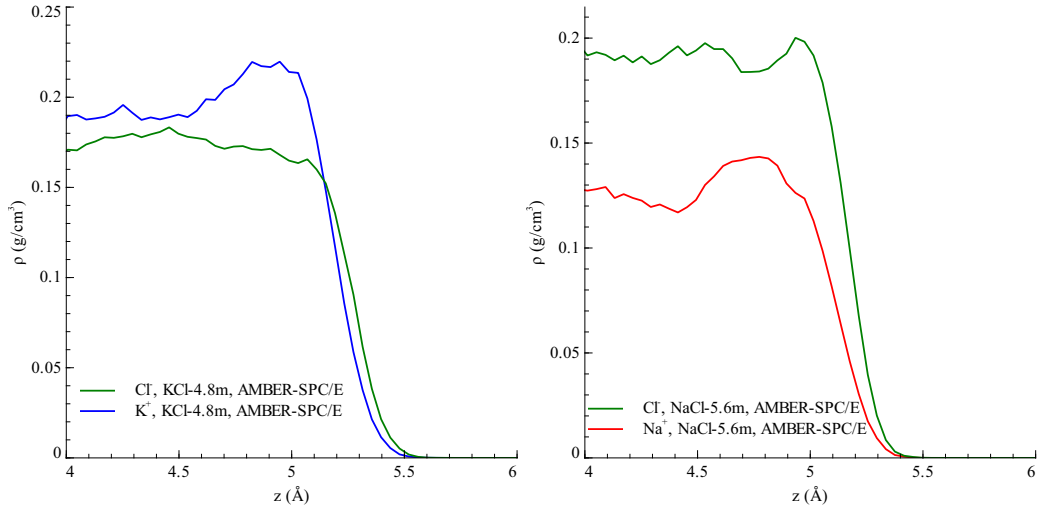


Figure S3: Density profiles for $K^+$ and $Cl^-$ ions in KCl solution at 4.8 m and for $Na^+$ and $Cl^-$ ions in NaCl solution at 5.6 m calculated with the newly developed AMBER-SPC/E potential [1].

112:9020–9041, 2008.

[2] J. Barthel, R. Buchner, and M. Münsterer. *Electrolyte Date Collection, Part2: Dielectric Properties of Water and Aqueous Electrolyte Solutions*. Dechema: Frankfurt, 1995.

[3] V. P. Sokhan and D. J. Tildesley. The free surface of water: molecular orientation, surface potential and nonlinear susceptibility. *Mol. Phys.*, 92:625–640, 1997.

[4] E. Harder and B. Roux. On the origin of the electrostatic potential difference at a liquid-vacuum interface. *J. Chem. Phys.*, 129:234706, 2008.

[5] S. E. Feller, R. W. Pastor, A. Rojnuckarin, S. Bogusz, and B. R. Brooks. Effect of electrostatic force truncation on interfacial and transport properties of water. *J. Phys. Chem.*, 100:17011–17020, 1996.

[6] P. Hunt and M. Sprik. On the position of the highest occupied molecular orbital in aqueous solutions of simple ions. *ChemPhysChem*, 6:1805–1808, 2005.

[7] S. M. Kathmann, I-F. W. Kuo, and C. Mundy. Electronic effects on the surface potential at the vapor-liquid interface of water. *J. Am. Chem. Soc.*, 130:16556–16561, 2008.

[8] W. R. Fawcett. The ionic work function and its role in estimating absolute electrode potentials. *Langmuir*, 24:9868–9875, 2008.